Reprinted from MONTHLY WEATHER REVIEW, Vol. 118, No. 8, August 1990
American Meteorological Society

A Heat Budget Analysis of the Polar Troposphere in and around Alaska during the Abnormal Winter of 1988/89

H. L. TANAKA AND MARY F. MILKOVICH

Geophysical Institute, University of Alaska Fairbanks, Fairbanks, Alaska

(Manuscript received 21 August 1989, in final form 16 February 1990)

ABSTRACT

In this study, we carried out a quantitative heat budget analysis of the polar troposphere in and around Alaska for the winter of 1988/89. The winter was characterized by drastic temperature variations. The surface minimum temperatures in the interior of Alaska were lower than −40°C during two weeks in late January. This cold period was followed by extremely warm weather during February, especially in northern Alaska.

The results of the heat budget analysis for the three-month average (December to February) show that the heat energy of the continental air mass in and around Alaska is maintained by a balance of warm advection, adiabatic warming, and radiative cooling. The analysis of the long-term variation during this period shows that the severe cold in late January was caused by an anomalous reduction in warm advection of sensible heat. The abnormally warm weather in February was caused by enhanced warm advection associated with a blocking formation over the North Pacific. We find that strong adiabatic warming due to large-scale descending motions occurs as a precursor to the blocking formation and the warm advection. It is suggested that the unusual temperature variation during this winter was caused by the enhanced, low-frequency variation of the large-scale flow. The local radiative cooling acts to reduce the rapid temperature variation due to advection change.

1. Introduction

Continental polar air masses are characterized by the presence of deep and persistent surface inversions, caused primarily by radiative cooling (e.g., Petterssen 1956). The modification of maritime polar air into continental polar air during winter was discussed by Curry (1983), using one-dimensional numerical model simulations. The model includes physical processes of surface enthalpy flux; infrared radiative cooling due to emission by CO_2, water vapor, water droplets, and ice crystals; gravitational settling of the condensed water; turbulent mixing; and subsidence. The numerical experiments shows that the formation of continental polar air is dominated by the radiative cooling due to emission by ice crystal and water droplets suspended in the cooling air. The continental air acquires most of the polar air mass properties after only four days by these processes. The results are consistent with the previous theoretical investigation by Wexler (1936).

In Curry (1987), the numerical experiment is further expanded to two-dimensional models, including a circular symmetric meridional circulation. For the formation of the polar continental air near 80°N, Curry proposed the importance of a positive feedback loop between condensation in the cooling air and the direct meridional circulation. The condensation enhances the radiative cooling of the air, while the subsidence due to the meridional circulation feeds more moisture aloft into the boundary layer. The cooling is ultimately limited by heat flux through the snow/ice and by the reduction of radiative cooling. The dominant downward motion is predicted by this model for cold-core anticyclones near Alaska, Siberia, and Greenland. This simple model, however, imposes a rigid wall at the southern boundary of polar region, ignoring the meridional heat transport from middle latitudes. Recent quantitative analysis by Nakamura and Oort (1988) showed that heat energy of the winter polar air mass (70°–90°N) is maintained by a balance of radiative cooling (157 W m^{-2}) and cross-boundary heat flux from the lower surface (48 W m^{-2}) and from lower latitudes (108 W m^{-2}). Such a large meridional heat transport is accomplished mainly by transient and stationary waves. Therefore, the results from simple dynamics including only the symmetric meridional circulation by Curry may not adequately describe the characteristics of the continental polar air. More observational support is necessary.

Colucci (1985), on the other hand, discussed formation of warm-core anticyclones identified as blocking highs. Colucci concluded that the observed temperature increase in the blocking anticyclones is forced both by warm air advection and subsidence warming, while the temperature decrease observed in the *blocking cyclones* is forced by adiabatic cooling caused by strong ascending motions. These blocking cyclones and anticyclones occur frequently in high latitudes near

Corresponding author address: Dr. H. L. Tanaka, Geophysical Institute, University of Alaska–Fairbanks, Fairbanks, AK 99775-0800.

Alaska, the North Atlantic, and Greenland. Note that the temperature decrease is associated with strong upward motions, which contrasts greatly with the downward motions in Curry's polar continental air. Therefore temperature variations in high latitudes are not simple, and further observational analyses are necessary to understand the properties of polar continental air.

The Alaska winter of 1988/89 was unusual with respect to the drastic temperature variation. A number of new record low temperatures at the surface were reported in interior Alaska at the end of January. Among these new records were −60.0°C at Tanana and −59.4°C at McGrath. (The all-time state record is −62.2°C set in 1971 at Prospect Creek.) In the beginning of February, this extremely cold air mass in the lower troposphere over Alaska began to slide southeast through Canada to the northern United States. As the cold air mass passed through these regions, many new record low temperatures were set. In contrast to the cold conditions developing in the northern United States, Alaska warmed dramatically in early February. During this time, a warm maritime air mass was transported over Alaska via enhanced meridional flow induced by pronounced atmospheric blocking over the North Pacific. The maritime warm air was combined with a strong downslope flow over the Alaska Range and Brooks Range to produce very warm monthly mean surface temperatures at Fairbanks and Barrow. The monthly mean temperature at Barrow was 18°C warmer than normal. The surface temperature variations in January and February 1989 for Barrow and Fairbanks, Alaska, are shown in Fig. 1. The 1989 winter included two weeks of temperatures below −40°C in late January at both locations. We realize that the 1989 cold spell was a long and intense one in comparison to those in recent years, however, the anomalously warm monthly mean temperature for February at Barrow was more than four times greater than the standard deviation of the long-term February mean at Barrow (see Walsh and Chapman 1990). The quantitative heat budget analysis of the unusual winter 1988/89 in and around Alaska offers a good opportunity to investigate the formation and destruction of a polar air mass.

The objective of the present study is to conduct a quantitative assessment of the extreme temperature variation of the polar troposphere in and around Alaska during the abnormal winter of 1988/89. The questions to be addressed include: Why did the persistent cold snap occur? Why was the cold spell suddenly replaced by an abnormal warm spell in February? How did thermodynamic terms vary associated with the extreme temperature variation? In order to answer these questions, we first analyzed the horizontal and vertical extension of the rapid temperature variations. It will be shown that the temperature variation is not confined to the lower troposphere, instead it is an entire tropospheric phenomenon in and around Alaska. We then performed a quantitative heat budget analysis over the analysis domain in the troposphere, using upper air meteorological data provided by the National Meteorological Center (NMC). We examined the time series and the vertical structures of the fundamental thermodynamic terms. The results of this heat budget analysis will show the most prominent thermodynamic term responsible for the extreme variation in temperature during the winter of 1988/89.

The dataset used in this heat budget analysis and the governing thermodynamic equation are described in section 2. Section 3 describes the large-scale circulation patterns and temperature distributions used to determine the analysis domain. The results of the heat budget for the specific analysis domain are presented in section 4. Finally, a concluding summary is given in section 5.

2. Data and scheme of analysis

We obtained the NMC grid-point global analysis data for the period of 1 December 1988 through 28 February 1989 from the National Center for Atmospheric Research. The dataset contains twice daily (0000 and 1200 UTC) meteorological variables of horizontal wind, temperature, geopotential, and humidity on the 2.5° × 2.5° longitude–latitude grids at the mandatory vertical levels of 1000, 850, 700, 500, 400, 300, 250, 200, 150, 100, 70 and 50 mb. The original data on the 2.5° × 2.5° grid for the twelve vertical levels were reduced to a 5° × 5° grid with 37 latitudes from 90°S to 90°N and 72 longitudes eastward from 0° (Greenwich) to 360°.

A vertical p-velocity ω ($=dp/dt$) was estimated kinematically based on mass continuity with the application of a horizontal plane-fitting method and a quadratic correction at the top of the atmosphere (see O'Brien 1970; Kung 1972). The small-scale divergence field is filtered by the plane-fitting method. The surface value of ω was estimated from the geopotential tendency with an assumption of vanishing vertical wind, w ($=dz/dt$) = 0, near the surface. Under the strong temperature inversion of polar winter, the surface horizontal wind is also negligibly small: $V \approx 0$. These assumptions of vanishing winds near the surface allow us to estimate the surface omega, ω_s by (e.g., Tanaka and Kung 1988)

$$\omega_s \approx \frac{p_s}{RT_s}\frac{\partial \phi_s}{\partial t}, \qquad (1)$$

where the subscripts s denote the values at the surface.

Day and Morone (1985) described the NMC data analysis procedure in terms of a fully multivariate optimum interpolation scheme. They discussed the error range of the wind analysis. The reasonableness and consistency of the analysis data were evaluated by a cross-section of the zonally averaged v component of the wind. A comparison of the analysis data and the

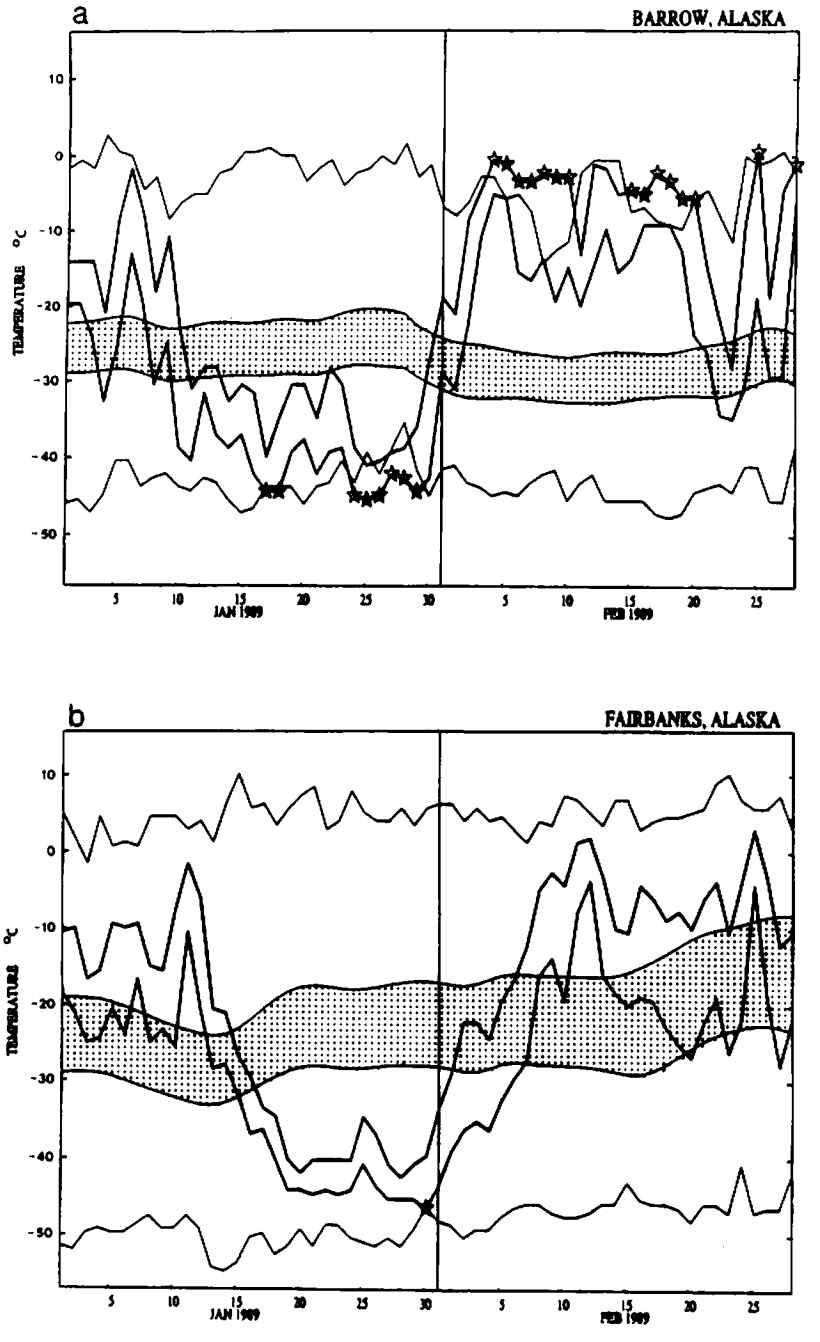

FIG. 1. Time series of daily high and low temperatures (thick lines) during January and February 1989 at (a) Barrow, Alaska (71.3°N, 156.8°W) and (b) Fairbanks, Alaska (64.8°N, 147.9°W). The shaded area denotes the 30-year (1951–80) normal and the upper and lower thin lines denote the record temperatures during the 30 years. The new records are marked by star symbols.

initialized data reveals that at low levels the direct and indirect circulations are virtually unchanged. The results suggest, at least in part, the acceptable quality of the NMC data. In Kung and Tanaka (1983) the quality of the kinematic estimation of ω by the NMC wind data was compared with the ω fields analyzed by the European Centre for Medium Range Weather Forecasts (ECMWF) and by the Geophysical Fluid Dynamics Laboratory (GFDL) during the First GARP Global Experiment (FGGE). Their results of eddy baroclinic conversion for the NMC data were comparable to those for the ECMWF, but were smaller than those for the GFDL. Although the vertical motion is anticipated to contain a large fraction of error, the

estimated vertical motion seems to contain meaningful signals. In this study an adequate averaging over a wide domain and a long period is performed in order to increase the reliability of the analysis result. The 5° × 5° grid analysis data including the diagnostically-computed ω field constitute the basic input data for the computation of the heat budget analysis in the following sections.

Using a pressure coordinate in the vertical direction, the first law of thermodynamics represented by enthalpy (c_pT) may be written as

$$\left[\frac{\partial c_pT}{\partial t}\right] = [-\mathbf{V}\cdot\nabla c_pT] + \left[\frac{c_p\gamma}{p}\omega\right] + [Q], \quad (2)$$

where the symbols denote temperature T, horizontal wind vector $\mathbf{V}$, vertical p-velocity ω, pressure p, time t, specific heat at a constant pressure c_p, and diabatic heating rate Q (involving radiative processes, vertical flux of sensible heat, and latent heat release, among others). A static stability parameter γ is defined as in Tanaka and Kung (1988):

$$\gamma = \frac{RT}{c_p} - p\frac{\partial T}{\partial p}, \quad (3)$$

where R is the gas constant of dry air. The bracket in (2) denotes a mass integral operator over a locally-defined atmospheric domain:

$$[\cdot] = \frac{1}{gA}\int_A\int_{p_t}^{p_s}(\cdot)dpdA, \quad (4)$$

where g is the earth's gravity and A represents a closed horizontal area over an isobaric surface. We used p_s = 1000 mb and p_t = 300 mb for the bottom and top of the analysis domain in this study.

According to (2), a temperature variation represented by c_pT is caused by the three terms appearing on the right-hand side: a horizontal advection of sensible heat, an adiabatic expansion or compression due to vertical motion, and diabatic processes including radiative heating. In the present study, the diabatic term has been evaluated by a residual balance of the heat budget equation (2). Since latent heat release and shortwave radiation appear to be small in the extremely cold, high-latitude environment, the residual term $[Q]$ may be considered to be primarily radiative cooling due to longwave radiation toward outer space. Vertical flux of sensible heat from the ground may be a secondary effect because the surface snow cover over the continent behaves as an efficient insulator.

3. Large-scale circulation pattern and the analysis domain

Large-scale flow patterns at the 500 mb level are presented in Fig. 2 for time averages of the period 1–15 January, 16–31 January, and 1–15 February. These three charts of geopotential height describe the general flow pattern for the period before, during, and after the severe cold in Alaska.

Before the severe cold (Fig. 2a), an upper air trough developed around the western Pacific sector, and a ridge developed over Alaska. There was southwesterly flow over the Bering Sea. The 500 mb flow pattern near Alaska is similar to the normal January pattern. During the extreme cold in Alaska (Fig. 2b), the flow pattern is very zonal over the north central Pacific. The previous southwesterly flow over the Bering Sea became northwesterly for this cold period. The flow realized is a typical pattern of high zonal index in the Pacific sector. After two weeks of the cold spell, a large and persistent blocking pattern developed over the North Pacific. The anomalously low zonal index pattern, indicating a strong ridge near Alaska, was combined with the cold and dense air mass remaining above the surface. This caused a record-breaking high sea-level pressure condition in interior Alaska. (A sea-level pressure of 1078.4 mb was observed at Northway, Alaska, on 31 January, which is a new high record in North America.) The cold air mass at the lower troposphere moved southward to the northern United States through Canada in February. During this time, a warm maritime air mass associated with the strong and persistent meridional flow was transported to western Alaska.

Figure 3 illustrates Northern Hemisphere temperature distributions at the 700 mb level for the average time periods corresponding to the 500 mb charts in Fig. 2. Before the extreme cold in Alaska, the coldest air mass was located over East Siberia (Fig. 3a). The temperature of the air mass was below −30°C. The 700 mb contours over the North Pacific, Aleutians and Alaska are approximately parallel to the 500 mb contours. Apparently, as the figure indicates, Alaska is warmer than East Siberia at 700 mb level. During the latter half of January, the −30°C contour expanded eastward to encompass Alaska, Northwest Territories, and Greenland (Fig. 3b). The figure shows the 700 mb temperature over Alaska to be as cold as that over the Arctic Ocean. After the cold spell, the −30°C contour contracted eastward to include Greenland alone (Fig. 3c).

The analysis domain of the present heat budget analysis has been determined by observing a characteristic horizontal extension of the temperature variation. Figure 4 describes the 700 mb temperature changes for the cooling period (difference between Figs. 3a and 3b) and the warming period (difference between Figs. 3b and 3c). As seen from Fig. 4a, a substantial cooling occurred in January in and around Alaska. The maximum cooling was about 12°C over interior Alaska. The horizontal extension of the −6°C contour encloses an area of 55°–80°N and 180°–100°W. In contrast, the temperature increase in February was even more striking. The maximum warming occurred over

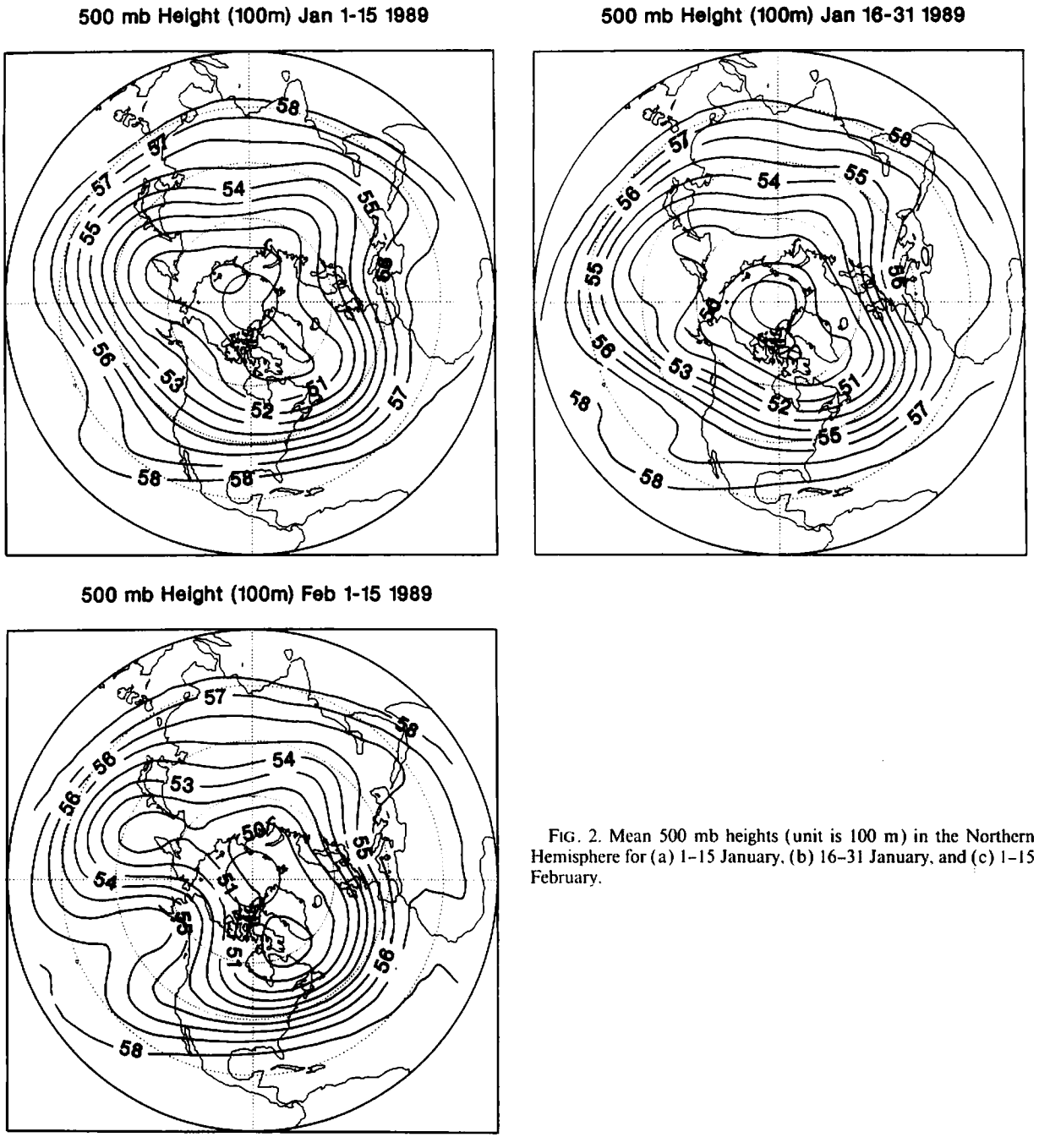

FIG. 2. Mean 500 mb heights (unit is 100 m) in the Northern Hemisphere for (a) 1–15 January, (b) 16–31 January, and (c) 1–15 February.

interior Alaska, showing a temperature increase of 20°C. The horizontal extension of the +10°C contour encloses an area of 50°–80°N, 160°E–110°W. With those results in mind, we set the domain of the present heat budget analysis to be a closed area of 55°–75°N, 110°W–180°, as is shown by the shaded area in Fig. 4.

First, the three-month (90 days) analysis period was divided into nine subperiods of 10-day length starting from 1 December 1988. We will call the nine subperiods early, mid, and late December and so forth, for convenience. The early January (31 Dec–9 Jan), and mid-January (10–19 Jan) subperiods are referred to collectively as a cooling period. Late January (20–29 Jan) corresponds to the severe cold in Alaska, and the subsequent periods of early February (30 Jan–8 Feb) and mid-February (9–18 Feb) subperiods are referred to as an abnormal warm period.

Vertical temperature profiles over the analysis domain are presented in Fig. 5 for sequential 10-day averages beginning in early January and ending in mid-February. Consistent temperature changes occur

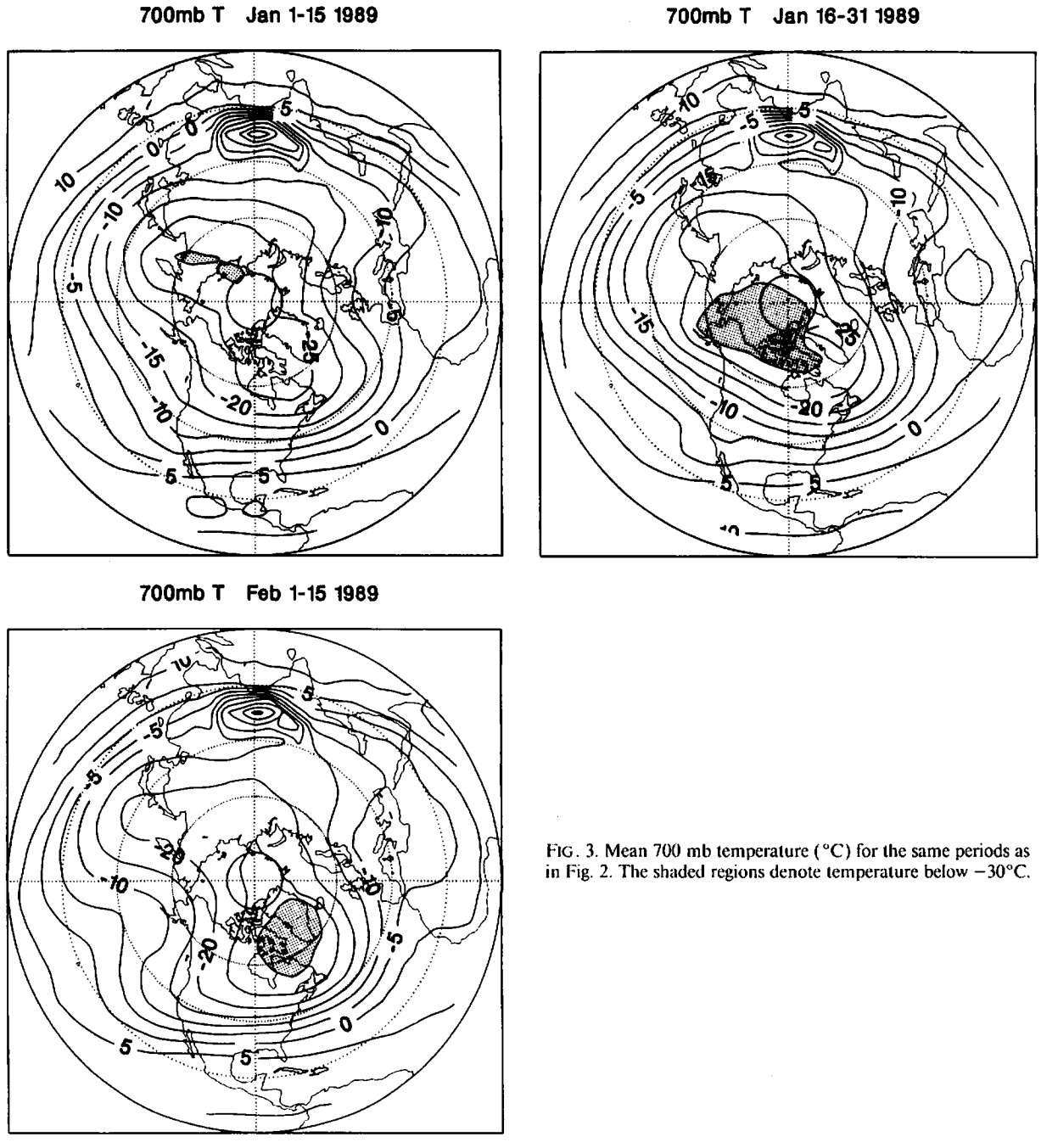

FIG. 3. Mean 700 mb temperature (°C) for the same periods as in Fig. 2. The shaded regions denote temperature below −30°C.

throughout the troposphere. The temperature changes are opposite in the stratosphere. Therefore, it is clear that the severe cold in Alaska and the subsequent warming were not confined to the lower troposphere but, in fact, extended throughout the troposphere. There are also commonly observed temperature inversions present below the 850 mb level as a result of a predominant radiative cooling at the surface.

The domain-averaged static stability parameter γ (Fig. 6) indicates the maximum near the surface and the minimum near the 500 mb level. The time variation shows that γ increases near the tropopause during the cooling period, but the variation is small near the surface.

The corresponding ω profiles are illustrated in Fig. 7. Since ω was negative during January, there was an ascending motion for the domain average. Then ω became strongly positive in early February, compressing the air by downward motion. The ω values decreased in mid-February. The time variation of ω seems to be consistent with the actual temperature change, although a comprehensive understanding of the change

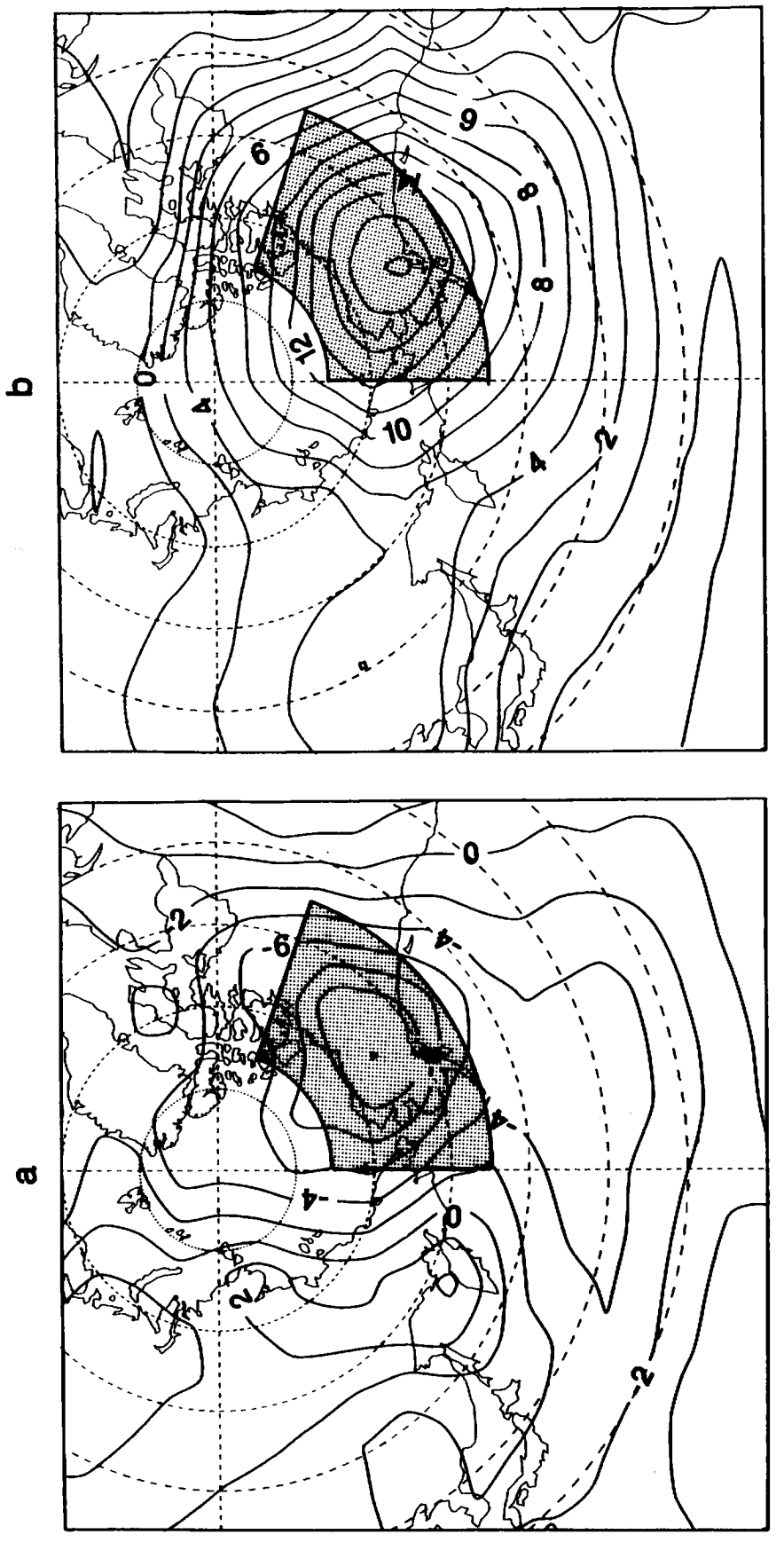

FIG. 4. Temperature changes (a) for the cooling period (difference between Figs. 3a and 3b) and (b) for the warming period (difference between Figs. 3b and 3c). The contours are at 2°C intervals. The hatched area (55–75°N, 110–180°W) represents the analysis domain for the present heat budget.

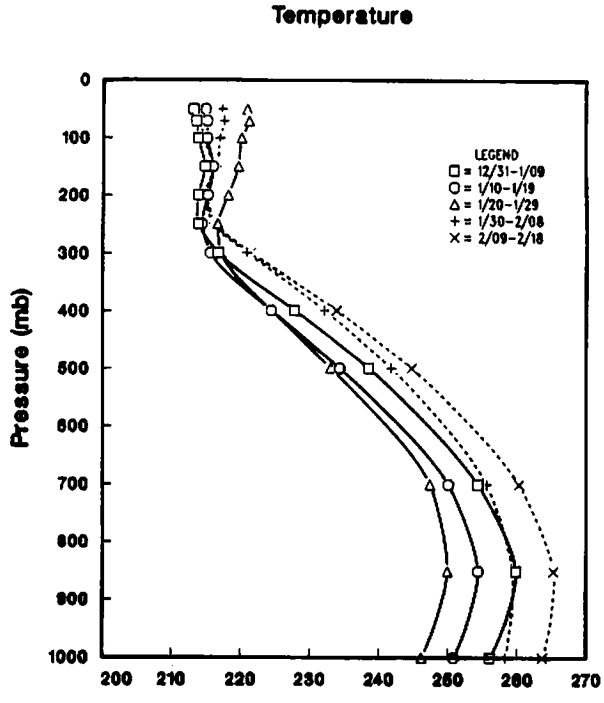

FIG. 5. Vertical temperature profiles over the analysis domain for 10-day averages of 31 Dec–9 Jan (square), 10–19 Jan (circle), 20–29 Jan (triangle), 30 Jan–8 Feb (plus), and 9–18 Feb (cross). The solid lines denote the cooling period, and dotted lines the warming period. The unit is kelvins.

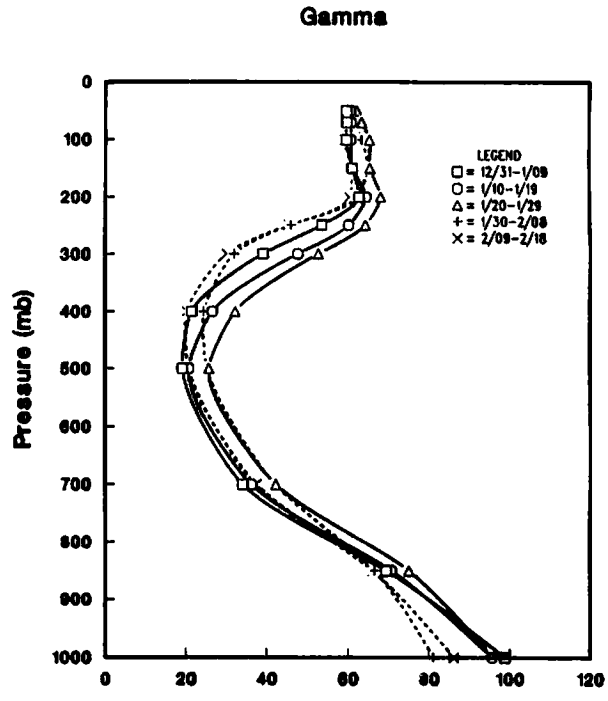

FIG. 6. Vertical profiles of static stability parameter γ over the analysis domain for 10 day averages as in Fig. 5. The unit is Kelvins.

requires knowledge of other thermodynamic terms. The diagnostic results of ω are quite different from numerical model experiments by Curry (1987), which infer a prevailing downward motion in the development of a cold-core air mass by radiative cooling.

4. Results of the heat budget

a. Time series

The results of the heat budget calculations are presented in this section for the severe cold in the latter half of January and the subsequent abnormal warm weather in February. Figure 8a shows a time series of enthalpy integrated over the analysis domain defined in Fig. 4. The 5-day running mean of the time series is also presented by thick lines. Temporal variations are superimposed on the low-frequency variation. The enthalpy decreases from a peak in mid-December to a minimum in late January. It increases rapidly at the beginning of February and remains at a high level during the month. The time series for the entire tropospheric change reasonably reflects Alaska's severe cold near the surface during the latter half of January and the subsequent abnormal warm weather in February. Hence, the examination of the tropospheric heat budget for the tropospheric integral appears to be the most meaningful method of assessing the unusual temperature variation change during the winter 1988/89.

The time series of the thermodynamic terms appearing in the heat budget equation (2) are presented in Fig. 8. The sensible heat advection is, in general, positive, thereby raising the temperature. About 100

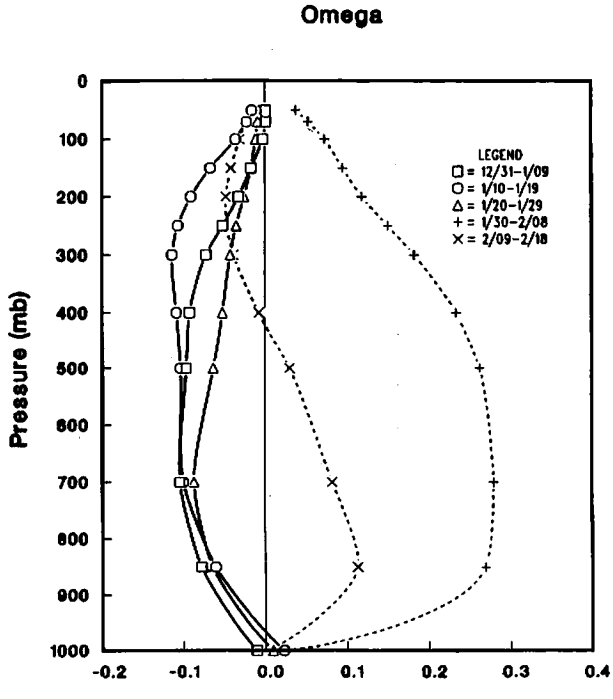

FIG. 7. Vertical profiles of ω over the analysis domain for 10 day averages as in Fig. 5. The units are $\mu b\ s^{-1}$.

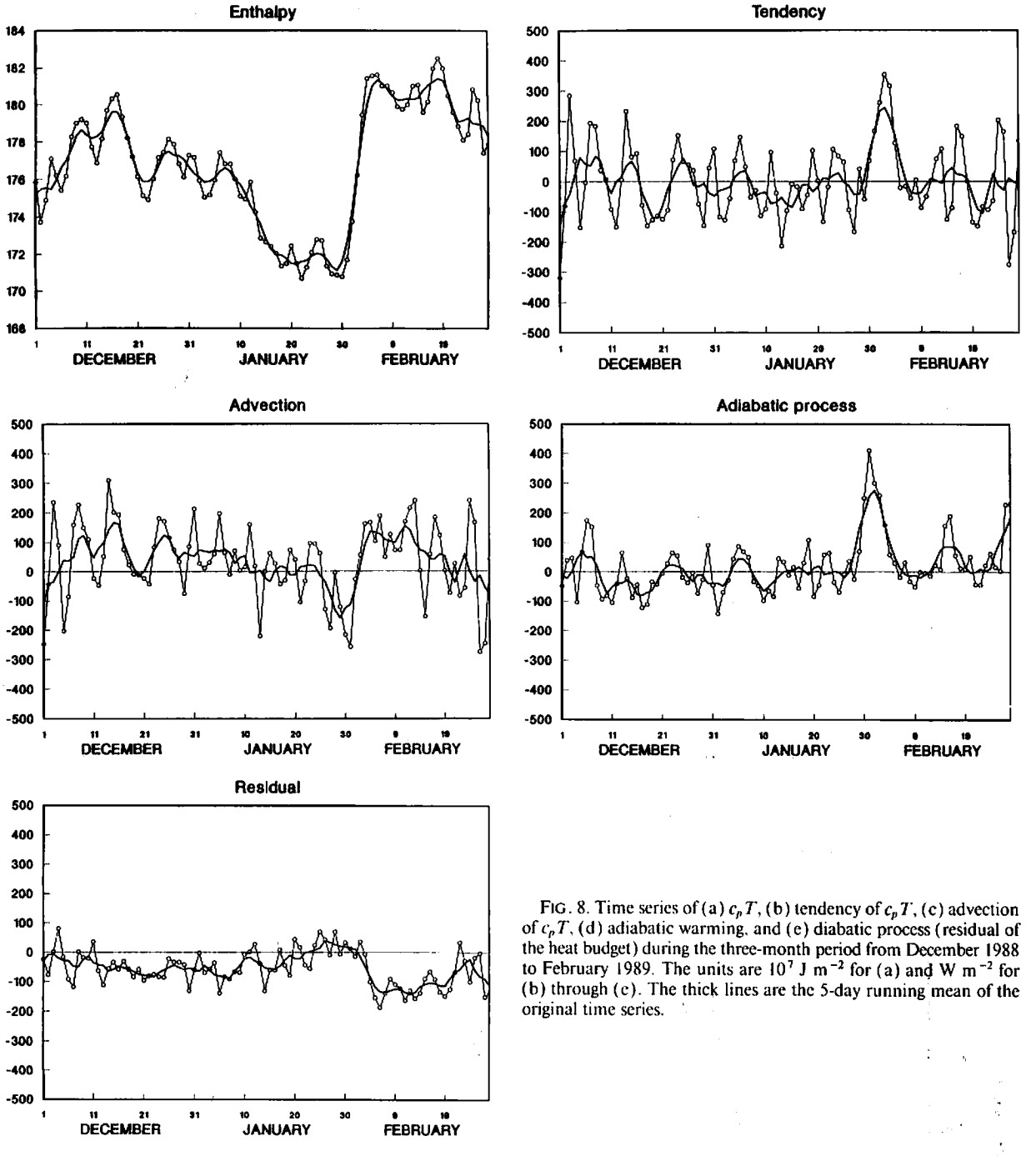

FIG. 8. Time series of (a) c_pT, (b) tendency of c_pT, (c) advection of c_pT, (d) adiabatic warming, and (e) diabatic process (residual of the heat budget) during the three-month period from December 1988 to February 1989. The units are 10^7 J m^{-2} for (a) and W m^{-2} for (b) through (e). The thick lines are the 5-day running mean of the original time series.

W m^{-2} of heating occurs before the cold spell. The advection decreases in January, and it becomes negative at the end of January. In February, the advection increases rapidly as meridional flow due to the blocking formation dominates. Adiabatic warming due to vertical motions provides a relatively small contribution except for during the period at the end of January. When the cold spell ended, strong adiabatic warming in excess of 300 W m^{-2} occurred, and the Pacific blocking formed. This increase in adiabatic warming accounts for the major warming as seen in the tendency term. The extraordinary sea-level pressure of 1078.4 mb was recorded during this period. It should be noted that the adiabatic warming due to the vertical motion occurred before the advective warming in the present case study. The blocking developed during the occurrence of significant downward motion over the domain as discussed by Colucci (1985). The residual of the heat budget is expected to be negative since it represents a dominant radiative cooling of the air column. The

results are consistent with the expectation, except for the period of late January. The short-term variations in the residual are considerably small in comparison to the other terms. The cooling is reduced during the cold spell and is enhanced during the warm spell; thus agreeing with the nature of longwave radiation. Since a temperature profile tends to approach an equilibrium profile, the radiative cooling is strong when it is warm, but the cooling is weak when it is cold.

b. *Vertical structures*

Figure 9 illustrates time changes in the vertical structure of the heat budget terms for the subperiods from early January till mid-February. In early January,

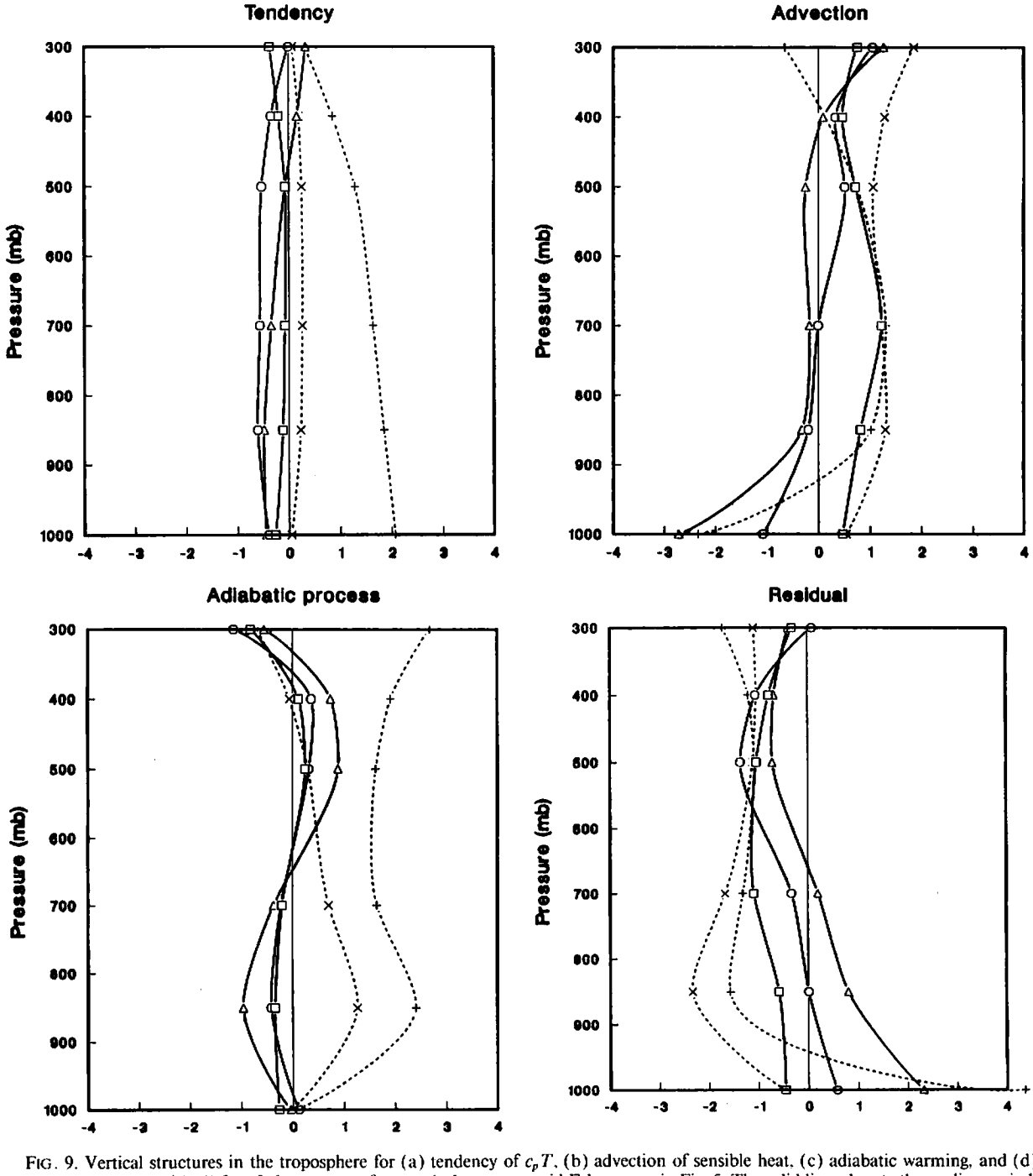

FIG. 9. Vertical structures in the troposphere for (a) tendency of c_pT, (b) advection of sensible heat, (c) adiabatic warming, and (d) diabatic processes (residual) for 10-day averages from early January to mid-February as in Fig. 5. The solid lines denote the cooling period, and dotted line the warming period. The units are °C day^{-1}.

a moderate cooling by longwave radiation takes place, and the warm air advection that compensates for the radiative coolings dominates the entire troposphere. During the severe cold, the advective warming is weakened considerably, and cold air advection occurs near the surface. The residual term indicates a positive value near the surface, which balances the cold air advection. Similar positive heating is seen near the surface in the data analyses by Mizzi and Kasahara (1989) or Fortelius (1989).

The severe cold ended with the enhanced adiabatic warming by descending motion in early February, and the increase of warm advection followed. The advective warming occurred in the layer of 400–850 mb. The radiative cooling increases everywhere except for the boundary layer.

These results indicate that the cold air advection near the surface plays an important role in the severe cold event in Alaska. The ascending motion accelerates the cooling in the lower troposphere. Net radiative cooling of the air occurs mainly above the inversion, and is considered to be a secondary effect of the abnormal temperature variation.

c. *Heat budget*

The results of the present heat budget are summarized in Table 1 for three-month averages and also for 10-day averages of the subperiods in the analysis. For the three-month statistics, we find that the advective warming ($-\mathbf{V}\cdot\nabla c_pT = 36$ W m^{-2}) and the adiabatic warming due to descending motion ($c_p\gamma\omega/p = 19$ W m^{-2}) are balanced by the radiative cooling (i.e., residual term, $Q = -54$ W m^{-2}).

For the 10-day averages in early January before the severe cold, the advection is 67 W m^{-2} and the residual is -67 W m^{-2}. The notable reduction of advective warming (from 67 to -29 W m^{-2}) is consistent with observed major cooling. Note that the radiative cooling is not the essential factor for the characteristic variation because it is rather weakened relative to the three-month average. During the severe cold, the contribution from the warm advection has vanished. The enhanced descending motion (145 W m^{-2}) leads to the outbreak of a warm period in early February. The large advection (98 W m^{-2}) in mid-February compensates the radiative cooling (-119 W m^{-2}).

The parentheses in Table 1 list the deviations of the heat budget term from its three-month mean. The results describe the key variable for the rapid temperature variation. It is found that the severe cold is caused by the anomalous reduction of warm air advection and by the cooling due to the persistent ascending motion. The radiative cooling seems to act oppositely to relax the variation. On the other hand, the abnormal warm spell is induced by the enhanced adiabatic warming and subsequent warm air advection. The dominant meridional flow associated with the blocking formation was important in mid-February.

5. Concluding summary

The Alaska winter of 1988/89 was unusual with respect to the drastic temperature variation. The surface weather stations observed a warmer than normal December, two weeks of -40°C (or even lower) during January in interior Alaska, and an extremely warm February in northern Alaska. Analysis results show that the temperature variation is not confined to the lower troposphere, but it is an entire tropospheric phenomenon in and around Alaska. Based on the results of horizontal and vertical extensions of the rapid temperature variation, we have conducted a heat budget analysis for a closed domain of 55°–75°N, 110°–180°W in and around Alaska over 300–1000 mb. The results of the present heat budget analysis are summarized as follows:

TABLE 1. A summary of heat budgets over the analysis domain (see Fig. 5) for a three-month average from December to February and for 10-day averages for the subperiods. The variables are enthalpy c_pT, tendency of c_pT, advection of c_pT, adiabatic warming $c_p\gamma\omega/p$, and residual balance Q in the troposphere (1000–300 mb). The units are 10^7 J m^{-2} for c_pT and W m^{-2} for heat transformations. The value in parenthesis is the deviation from the three-month average.

Period	c_pT	$\partial c_pT/\partial t$	$-\mathbf{V}\cdot\nabla c_pT$	$c_p\gamma\omega/p$	Q
			Three-month average		
01 Dec–28 Feb	177	1	36	19	−54
			10-day average		
01 Dec–10 Dec	177	22	39 (+3)	11 (−8)	−28 (+26)
11 Dec–20 Dec	179	−29	76 (+40)	−54 (−74)	−51 (+3)
21 Dec–30 Dec	177	−1	60 (+24)	7 (−12)	−68 (−14)
31 Dec–09 Jan	176	−12	67 (+30)	−12 (−31)	−67 (−13)
10 Jan–19 Jan	173	−40	6 (−30)	−8 (−27)	−38 (+16)
20 Jan–29 Jan	172	−17	−29 (−66)	−4 (−23)	16 (+70)
30 Jan–08 Feb	178	120	35 (−1)	145 (+125)	−60 (−6)
09 Feb–18 Feb	181	17	98 (+62)	37 (+18)	−119 (−64)
19 Feb–28 Feb	179	−46	−26 (−62)	53 (+34)	−74 (−19)

1) A heat budget for the three-month average in and around Alaska is maintained by a balance of advective warming (36 W m^{-2}), adiabatic warming due to descending motion (19 W m^{-2}), and radiative process (residual term, −54 W m^{-2}).

2) The severe cold in Alaska during late January was induced by an anomalous reduction of warm air advection resulting from a persistent zonal flow pattern in the middle latitudes. Cold advection near the surface from Siberia accelerated the cooling. This result of cold advection from Siberia agrees well with the observational analysis by Bowling et al. (1968). It is important to note that the domain-averaged vertical motion was upward during the cooling period. The vertical motion indicates the characteristics of the blocking cyclone discussed by Colucci (1985). There was a persistent cooling due to the adiabatic expansion in the lower troposphere caused by a large-scale ascending motion.

3) The abnormal warm weather in February was caused by an enhanced adiabatic warming. The warm advection due to the strong meridional flow occurred after the adiabatic warming associated with a blocking formation in the North Pacific.

According to Nakamura and Oort (1988), the arctic air mass maintains its heat energy through a fundamental balance of radiative cooling and meridional heat transport from the south. The results of the three-month average in this study are qualitatively consistent with their results. When the long-term variations are concerned, our results showed that the unusual temperature variation during 1988/89 was caused by the variations of meridional heat transport. The diabatic process appears to act passively to reduce a rapid temperature variation due to the advection change. Therefore we suggest that the abnormal cold event in Alaska was induced by the unusually strong large-scale dynamical processes rather than anomalous radiative cooling due to the positive feedback between condensation and subsidence discussed by Curry (1987). Clearly, more case studies are necessary to assess the abnormal weather in Alaska.

Acknowledgments. The authors acknowledge Drs. G. Weller, G. Wendler, K. Stamnes, and S. A. Bowling for their useful suggestions. They are also indebted to the Alaska Climate Research Center and the National Weather Service Forecast Office at Fairbanks for providing important meteorological data, and the technical assistance rendered by C. Chafin. The research was supported by internal funds of the Geophysical Institute, University of Alaska Fairbanks.

REFERENCES

Bowling, S. A., T. Ohtake and C. S. Benson, 1968: Winter pressure systems and ice fog in Fairbanks, Alaska. *J. Appl. Meteor.*, **7**, 961–968.

Colucci, S. J., 1985: Explosive cyclogenesis and large-scale circulation changes: Implications for atmospheric blocking. *J. Atmos. Sci.*, **42**, 2701–2717.

Curry, J., 1983: On the formation of continental polar air. *J. Atmos. Sci.*, **40**, 2278–2292.

——, 1987: The contribution of radiative cooling to the formation of cold-core anticyclones. *J. Atmos. Sci.*, **44**, 2575–2592.

Dey, C. H., and L. L. Morone, 1985: Evolution of the National Meteorological Center global data assimilation system: January 1982–December 1983. *Mon. Wea. Rev.*, **113**, 304–318.

Fortelius, C., 1989: An intercomparison of residual energy budgets from atmospheric circulation data and satellite measurements of the earth's radiation balance. Dept. of Meteor., University of Helsinki. No. 32, 55 pp.

Kung, E. C., 1972: A scheme for kinematic estimate of large-scale vertical motion with an upper-air network. *Quart. J. Roy. Meteor. Soc.*, **98**, 402–411.

——, and H. Tanaka, 1983: Energetics analysis of the global circulation during the special observation periods of FGGE. *J. Atmos. Sci.*, **40**, 2575–2592.

Mizzi, A. P., and A. Kasahara, 1989: Intercomparison of daily values of atmospheric variables, including diabatic heating rates, from the ECMWF, GFDL, and Goddard Laboratory for Atmospheres FGGE level IIIb analyses. *J. Geophys. Res.*, **94**, 14 717–14 748.

Nakamura, N., and A. H. Oort, 1988: Atmospheric heat budget of the polar regions. *J. Geophys. Res.*, **93**, 9510–9524.

O'Brien, J., 1970: Alternative solutions to the classical vertical velocity problem. *J. Appl. Meteor.*, **9**, 197–203.

Petterssen, 1956: *Weather Analysis and Forecasting, Vol. 2.* McGraw Hill, 260 pp.

Tanaka, H. L., and E. C. Kung, 1988: Normal mode energetics of the general circulation during the FGGE year. *J. Atmos. Sci.*, **45**, 3723–3736.

Walsh, J. E., and W. L. Chapman, 1990: Short-term climatic variability of the Arctic. *J. Climate*, **3**, 237–250.

Wexler, H., 1936: Cooling in the lower atmosphere and the stratosphere of polar continental air. *Mon. Wea. Rev.*, **64**, 122–136.